Journal of Molecular Catalysis A: Chemical 313 (2009) 79–87

Contents lists available at ScienceDirect

Journal of Molecular Catalysis A: Chemical

journal homepage: www.elsevier.com/locate/molcata

L-Prolinamide functionalized mesoporous silicas: Synthesis and catalytic performance in direct aldol reaction

Jinsuo Gao, Jian Liu, Dongmei Jiang, Bing Xiao, Qihua Yang*

State Key Laboratory of Catalysis, Dalian Institute of Chemical Physics, Chinese Academy of Sciences, 457 Zhongshan Road, Dalian 116023, China

ARTICLE INFO

Article history:
Received 11 March 2009
Received in revised form 10 August 2009
Accepted 10 August 2009
Available online 15 August 2009

Keywords:
Mesoporous silicas
Aldol reaction
Chiral
Prolinamide

ABSTRACT

Mesoporous silicas functionalized with the L-prolinamide group in the mesopore were synthesized by co-condensation of silicon precursors with L-prolinamide modified organosilane (PCA) in HOAc–NaOAc buffer solution (pH = 4.4) using block copolymer P123 as a template. The highly ordered 2D hexagonal mesostructure was obtained through one-pot co-condensation of tetraethoxysilane (TEOS), Na_2SiO_3 and PCA as silicon source. The disordered foam-like mesostructure was also obtained when TEOS and PCA were used as silicon sources. In asymmetric aldol reaction of cyclohexanone with 4-nitrobenzaldehyde, the materials with highly ordered mesostructure exhibit higher enantioslectivity (91% ee) than that with disordered foam-like mesostructure (75% ee), suggesting that the ordered pore structure imparts improved enantioselectivity. The L-prolinamide functionalized materials were also synthesized by grafting PCA onto mesoporous silicas, which showed catalytic efficiencies similar to the materials synthesized by the co-condensation method.

1. Introduction

Recently, the asymmetric organocatalysis has blossomed rapidly and is recognized as the third important kind of asymmetric catalysis, thus complementing the well-established asymmetric transition-metal and enzyme catalysis processes. Unlike transition-metal catalysts, organocatalysts avoid the use of metals, which can be both expensive and toxic. Furthermore, organocatalysts are also much cheaper and easier to handle than the transition-metal complexes and enzyme [1–3]. A variety of key asymmetric carbon–carbon and carbon–heteroatom bond-forming reactions can be carried out by using organocatalysts. However, most reaction systems employing the organocatalysts generally need high catalyst/substrate ratios; in some cases, even higher than 30 mol% of organocatalyst is required. Moreover, the reactions are usually performed in homogeneous processes. In view of separation and recycling of the catalyst and purification of the product, the heterogeneous organocatalytic process is more desirable.

The incorporation of homogeneous catalysts onto solid support is widely used for heterogenization of asymmetric transition-metal complexes. However, only limited researches have been devoted to immobilization of organocatalysts and most works used polymer as support. Compared with polymer, inorganic supports with higher surface area and thermal stability are desirable support materials for immobilization of organocatalyst. Recently, Zhong et al. reported that L-proline adsorbed on γ-Al_2O_3 unexpectedly switched the enantioselectivity of the direct asymmetric reaction of acetone with *p*-nitrobenzaldehyde from 68% ee (R) to 21% ee (S) [4]. Yamaguchi et al. found that the N-octyldihydroimidazolium hydroxide fragment co-valently anchored on SiO_2 showed high catalytic performance for the cyanosilylation of various carbonyl compounds with trimethylsilyl cyanide [5]. Yu et al. reported that mesoporous silica supported 9-thiourea epi-quinine showed enhanced ee value in the asymmetric Friedel–Crafts reaction of imines with indoles [6]. The L-proline was also co-valently grafted onto MCM-41 [7]. Recently, L-proline was immobilized onto mesoporous silica through a direct synthesis method; it was found that the material having short channel with plugs in the pore structure showed higher enantioselectivity than the homogeneous counterpart in the diethyl malonate addition reaction [8].

In this paper, the organosilane precursor containing the L-prolinamide (PCA) group was synthesized because the previous studies showed that bifunctional L-prolinamide derivatives were highly efficient organocatalysts in the direct asymmetric aldol reactions [9]. The mesoporous silicas with the L-prolinamide functional group in the mesopores were synthesized by co-condensation of PCA with silicon precursors in mild buffer solution using block copolymer P123 as the template. The materials with SBA-15 and foam mesostructure were successfully synthesized using a mixture of TEOS and Na_2SiO_3 or pure TEOS as silicon precursors. For comparison, the PCA was also grafted onto SBA-15 and MCM-41. The catalytic properties were investigated in a direct asymmetric aldol reaction. The catalytic results showed that the materials

* Corresponding author. Tel.: +86 411 84379552; fax: +86 411 84694447.
E-mail address: yangqh@dicp.ac.cn (Q. Yang).
URL: http://www.hmm.dicp.ac.cn/ (Q. Yang).

1381-1169/$ – see front matter © 2009 Elsevier B.V. All rights reserved.
doi:10.1016/j.molcata.2009.08.005

with SBA-15 type mesostructure exhibited higher enantioselectivity than that with foam mesostructure. Compared with the grafting method, the co-condensation method could result in materials with L-prolinamide functional groups incorporated in higher amounts.

2. Experimental

2.1. Chemicals

The solvents were of analytical quality and dried by standard methods. Other materials were of analytical grades and used as received without further purification. Triblock copolymer P123 $[(EO)_{20}(PO)_{70}(EO)_{20}]$ was purchased from Sigma–Aldrich Company Ltd. 4-(Chloromethyl)phenyltrimethoxysilane (97%) was purchased from Gelest. Tetraethoxysilane (TEOS, 99%), sodium silicate solution (20% of SiO_2, 6% of Na_2O) and other reagents were obtained from Shanghai Chemical Reagent. N-[4-(trimethoxysilyl)benzyl]-(−)-(1R,2R)-diaminocyclohexane was synthesized according to the literature [10]. The supports of SBA-15 and MCM-41 for grafting were prepared according to the literature [11,12].

2.2. Synthesis

2.2.1. Synthesis of (2S, 1′R, 2′R)-N-t-butyloxycarbonyl-pyrrolidine-2-carboxylic acid [2′-(4-trimethoxysilylbenzylamide)-cyclohexyl] amide (PCA)

N-*t*-butyloxycarbonyl-L-proline (9.6 g, 40 mmol) and N,N′-dicyclohexylcarbodiimide (DCC) (9.3 g, 40 mmol) were dissolved in 80 mL of dichloromethane and cooled down to 0 °C. After stirring for 30 min, a solution of N-[4-(Trimethoxysilyl)benzyl]-(−)-(1R,2R)-diaminocyclohexane (16.7 g, 32 mmol) in 40 mL of dichloromethane was added dropwise over 15 min and the mixture was warmed to room temperature. After stirring for 24 h at room temperature, the reaction mixture was filtered and a yellowish viscous liquid corresponding to compound PCA was obtained after pumping off the solvent from the filtrate under vacuum. IR: ν 3428, 3323, 2941, 1702, 1670, 1398, 1119, and 793 cm^{-1}; ^1H NMR ($CDCl_3$, 400 MHz) δ (ppm) 1.2–2.9 (m, 27H, cyclohexyl, pyrrolidinyl, Boc, NH), 3.5–4.2 (m, 11H, $-(OCH_3)_3$, CH_2Ph), 7.1–8.0 (m, 5H, H_{arom}, NH—C=O); ^{13}C NMR (400 MHz, $CDCl_3$) δ (ppm) 23.6, 24.9, 26.2, 28.6, 29.3, 31.8, 32.9 ($3^{\#}$, $4^{\#}$, $5^{\#}$, $6^{\#}$ C of cyclohexyl, $3^{\#}$, $4^{\#}$ C of pyrrolidinyl and $(CH_3)_3$); 47.6, 50.4, 53.0, 54.6, 58.6, 60.8, 80.6 ($PhCH_2$, $1^{\#}$, $2^{\#}$ C of cyclohexyl, $2^{\#}$, $5^{\#}$ C of pyrrolidinyl, C—O of Boc and $(CH_3O)_3Si$); 126.5 127.8, 130.0, 142.4 (aromatic ring); 155.2, 172.8 (C=O); $[\alpha]^{29}_D = -5.6$ (C=0.56, $CHCl_3$); Elemental analysis: Anal. Calcd. for $C_{26}H_{43}N_3O_6Si$: C, 59.88; H, 8.25; N, 8.06. Found: C, 59.93; H, 8.09; N, 8.34.

2.2.2. Synthesis of mesoporous silicas with L-prolinamide functional group in the mesopore by co-condensation method

The mesoporous silicas were synthesized according to a modified method reported in our previous paper [13]. For a typical procedure, P123 (1.0 g) was dissolved in 28 mL of HOAc–NaOAc buffer solution (pH = 4.4, HOAc: 0.52 mol/L, NaOAc: 0.27 mol/L) at 25 °C and stirred for 20 h. To the above solution, 2 mL of sodium silicate aqueous solution (20% of SiO_2, 6% of Na_2O, weight ratio) was added. After 10 min, a mixture (8.5 mmol) of TEOS and PCA was added. The reaction mixture was stirred at 40 °C for 24 h and aged at 100 °C under static conditions for an additional 24 h. After filtration, the as-synthesized material was dried at 25 °C and the surfactant was extracted twice by refluxing 1.0 g of as-synthesized sample in a solution composed of 200 mL of ethanol and 1.5 g HCl (37 wt.%) for 24 h. The sample was denoted as SBA-15-n-Boc, where n (n = 10, 20, 30) is the molar percent of PCA/(PCA + TEOS + Na_2SiO_3).

Foam-10-Boc was synthesized under similar conditions except that only a mixture of TEOS and PCA (molar percent of PCA/(PCA + TEOS) = 10%) was used.

2.2.3. Synthesis of L-prolinamide functionalized mesoporous materials by the grafting method

After drying SBA-15 or MCM-41 (1.0 g) under vacuum at 120 °C for 4 h, PCA (0.5 g) in 20 mL of freshly distilled anhydrous toluene was added under Ar atmosphere. The mixture was refluxed under stirring for 24 h. After filtration, the powder product was washed with toluene and dried under vacuum at 60 °C. The obtained materials were denoted as G-SBA-15-Boc or G-MCM-41-Boc.

2.2.4. Deprotection of BOC from the solid materials

The sample (1.0 g) was stirred in 20 mL of CH_2Cl_2/TFA (4/1) for 2 h. After filtration, the solid material was dried at room temperature. The obtained material was stirred in 50 mL of tetramethylammonium hydroxide in methanol solution (0.2 M) for 1 h at room temperature. After filtration, the product was washed with ethanol, water, and ethanol and dried under vacuum at 60 °C. The samples obtained from SBA-15-n-Boc, Foam-10-Boc, G-SBA-15-Boc, and MCM-41-Boc were denoted as SBA-15-n, Foam-10, G-SBA-15, and G-MCM-41, respectively.

2.3. Characterization

X-ray diffraction (XRD) patterns were recorded on a Rigaku RINT D/Max-2500 powder diffraction system using Cu Kα radiation of 0.15406 nm wavelength. The nitrogen sorption experiments were performed at −196 °C on a Micromeritics ASAP 2020 system. Prior to the measurement, the samples were out-gassed at 120 °C for at least 6 h. The Brunauer–Emmett–Teller (BET) area was calculated from adsorption data in a relative pressure P/P_0 range of 0.05–0.25. Pore size distribution was determined from the adsorption branches using the Barret–Joyner–Halenda (BJH) method. Pore volume was estimated at a relative pressure P/P_0 of 0.99. Transmission electron microscopy (TEM) was performed using a FEI Tecnai G2 at an acceleration voltage of 120 kV. FT-IR spectra were collected with a Nicolet Nexus 470 IR spectrometer. ^{29}Si (79.4 MHz) MAS NMR experiments were recorded on a Varian infinity-plus 400 spectrometer with the following experimental parameters: 4.00-kHz spin rate, 2.00-μs π/4 pulse width. ^{13}C (100.5 MHz) CP-MAS NMR experiments were recorded on a Varian infinity-plus 300 spectrometer with the following experimental parameters: 4.00-kHz spin rate; 2.00-min contact time; 5.00-s pulse delay. Elemental analysis of C, H, N was performed on an Elementar Vario EL III. Chiral HPLC was performed on Agilent 1100 series with chiral column (Chiralpak AD-H column).

2.4. Catalytic reaction

In a typical procedure, desired amounts of the material (containing 0.075 mmol of L-prolinamide base on elemental analyses) were added to a glass tube, followed by addition of 0.5 mL of $CHCl_3$ and 0.5 mL of cyclohexanone. Then the mixture was placed in an ethanol bath (−25 °C). After stirring for 20 min, ice acetic acid (4.3 μL) was injected into the above mixture using a 10-μL microsyringe supplied by Agilent Technologies, followed by the addition of 4-nitrobenzaldehyde (0.019 g, 0.125 mmol). The reaction mixture was stirred at −25 °C for 4 days. The catalyst was filtered, washed with ethyl acetate. The organic layers were combined and concentrated in vacuo. The obtained mixture was purified by silica gel flash chromatography (petroleum ether/ethyl acetate = 3/1) to give the products as a white solid including both syn and anti products. ^1H NMR ($CDCl_3$, 400 MHz) of the product: δ = 1.3–1.5 (m, 1H), 1.4–1.8 (m, 2H), 1.8–1.95 (m, 1H), 2.0–2.2 (m, 1H), 2.2–2.5 (m, 1H), 4.0–4.2 (1H), 4.8–5.0 (1H), 7.4–7.6 (m, 2H), 8.2–8.3 (m, 2H) ppm. The enantiomeric excess (ee) was determined by HPLC with a Chiralpak AD-H column on Agilent 1100 series (80:20 hexane: 2-propanol), 0.5 mL/min; λ = 254 nm; anti-enantiomer t_R = 24 min

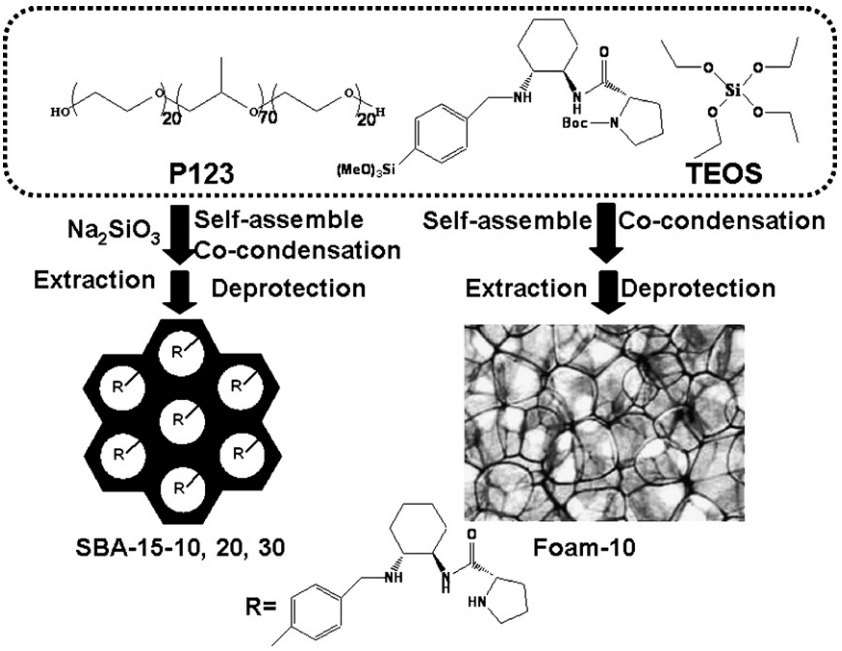

Scheme 1. Illustration of the synthesis of L-prolinamide functionalized mesoporous materials.

(minor) and t_R = 31 min (major); syn enantiomer t_R = 20 min (major) and t_R = 22 min (minor).

3. Results and discussion

3.1. Synthesis of L-prolinamide functionalized mesoporous silicas by co-condensation method

The mesoporous silicas could be synthesized under a wide range of pH values by using different kinds of templates, such as cationic, anionic, and nonionic surfactants, and block copolymers. Highly ordered mesoporous silicas with 2D and 3D hexagonal and cubic (*Pm*-3*n*, *Im*-3*m*, *Fm*-3*m*) mesophases have been synthesized under strongly basic or acidic conditions based on the electrostatic interaction between the silicates and the template aggregates [14]. However, because PCA has O=C—NH groups, which tend to decompose in strongly acidic or basic medium, the synthesis of mesoporous silicas functionalized with L-prolinamide group should be performed in weakly acidic or basic medium. The mild buffer solution (HOAc–NaOAc, pH = 4.4) was employed as reaction medium for the synthesis mesoporous materials. Based on our previous studies [13], pure TEOS and a mixture of TEOS and Na_2SiO_3 were used respectively for the synthesis of L-prolinamide functionalized materials with foam and 2D hexagonal mesostructures. For comparison, the L-prolinamide functionalized mesoporous silica was also synthesized by the grafting method. The detailed synthesis process was outlined in Scheme 1.

3.2. Structure characterization

The XRD patterns of all materials are shown in Fig. 1. The XRD pattern of SBA-15-10-Boc synthesized with 10 mol% of PCA showed three well-resolved peaks, which could be indexed as (1 0 0), (1 1 0), and (2 0 0) diffraction peaks of a 2D hexagonal mesophase. Two

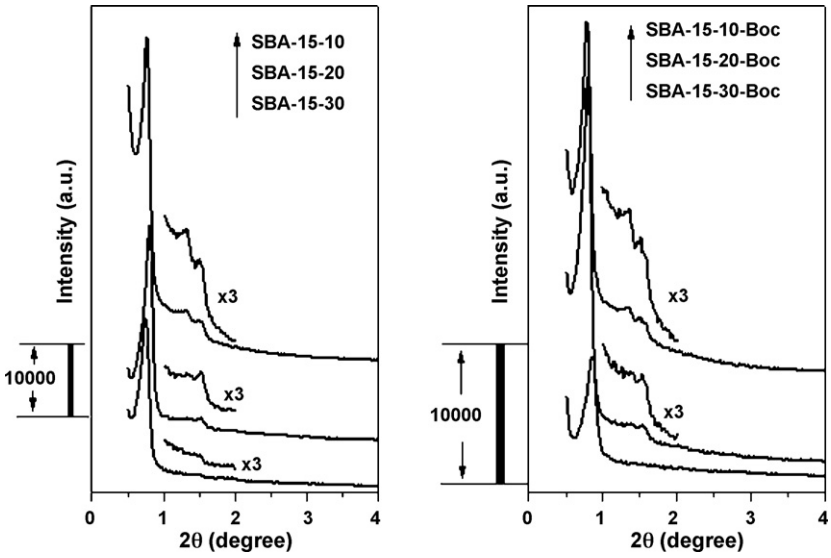

Fig. 1. XRD patterns of SBA-15-n-Boc and SBA-15-n.

Table 1
Textural parameters of L-prolinamide functionalized mesoporous materials[a].

Sample	d_{100} spacing (nm)	S_{BET} ($m^2\ g^{-1}$)	Volume[b] ($cm^3\ g^{-1}$)	Pore diameter (nm)	a_0[c] (nm)	Wall[d] thickness (nm)
SBA-15-10	11.6 (11.3)	378 (516)	0.86 (0.95)	9.2 (9.2)	13.4 (13.0)	4.2 (3.8)
SBA-15-20	11.1 (11.1)	305 (371)	0.51 (0.70)	7.2 (7.2)	12.8 (12.8)	5.6 (5.6)
SBA-15-30	11.9 (10.3)	152 (162)	0.22 (0.26)	6.0 (6.5)	13.8 (11.9)	7.8 (5.4)
Foam-10		464 (533)	1.09 (1.23)	28.3, 13.8 (41.8, 21.7)		
G-SBA-15	9.19 (8.68)	330 (602)	0.49 (0.88)	6.0 (8.0)	10.6 (10.0)	4.6 (2.0)
G-MCM-41	3.91 (3.77)	727 (844)	0.37 (0.70)	<1.7 (2.3)	4.5 (4.4)	>2.8 (2.1)

[a] Data in the parenthesis refer to the parameters of the samples before deprotection; for G-SBA-15 and G-MCM-41, data in the parenthesis refer to the parameters of the parent SBA-15 and MCM-41.
[b] Total pore volume obtained from the volume N_2 adsorbed at $P/P_0 = 0.99$.
[c] a_0 is the lattice parameter $a_0 = 2d_{100}/\sqrt{3}$.
[d] Wall thickness = a_0-pore diameter.

diffraction peaks were observed in the XRD pattern of SBA-15-20-Boc. For SBA-15-30-Boc synthesized with 30 mol% of PCA, only one relatively broad peak appeared in the low angle range in the XRD patterns, indicating that this material had less ordered mesostructure. The deterioration of the mesostructural ordering with the increase in the organosilane PCA content is a common phenomenon for the hybrid mesoporous materials synthesized by co-condensation of $RSi(OR')_3$ and $Si(OR')_4$ [15–18]. This may be due to the weakened interaction between the silica/organosilica oligomers and the PEO corona of P123, which was caused by the increased amount of organic groups and reduced density of silanol groups at the silica/template interface. SBA-15-n materials had XRD patterns similar to the parent SBA-15-n-Boc materials. It should be noted that the deprotection of the materials with 2D hexagonal mesophase provoked a relevant increase in the intensity of the (1 0 0) reflection. The significant increase in the diffraction intensity after deprotection may be caused by the increase in the contrast of the walls and pore due to the removal of the large Boc groups in

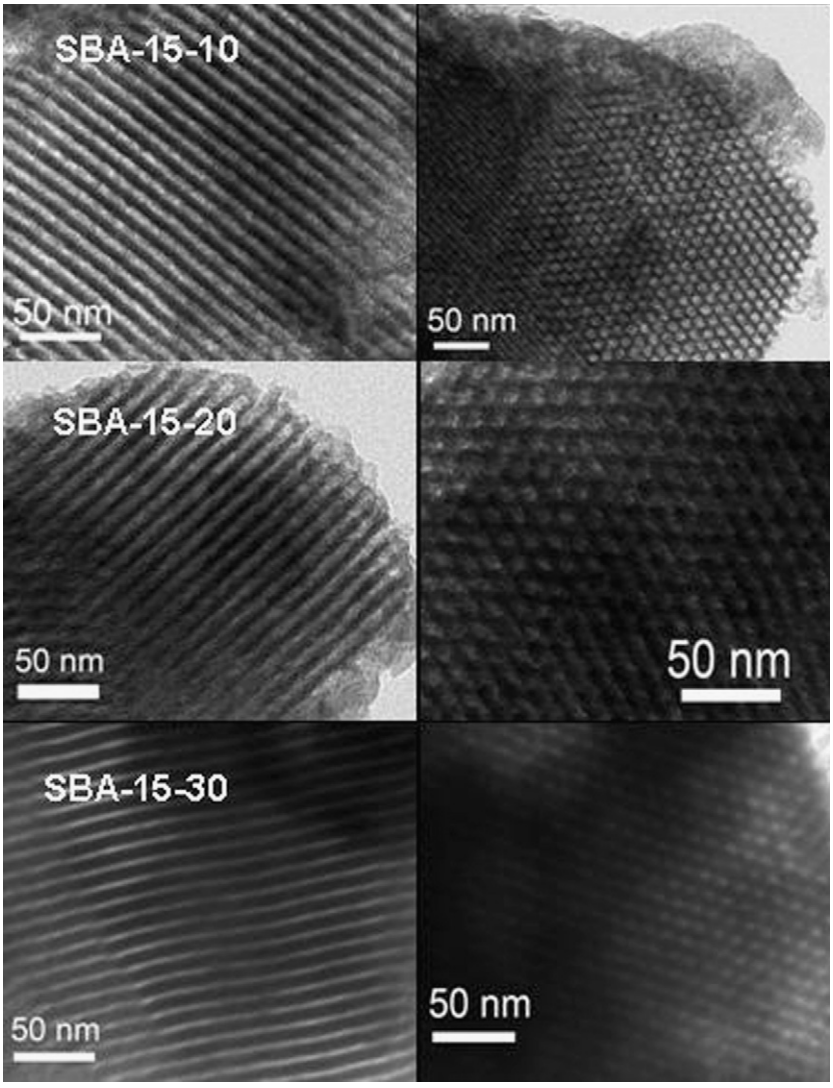

Fig. 2. TEM image of sample SBA-15-n with the incidence direction (left) perpendicular to the axis and (right) parallel to the axis.

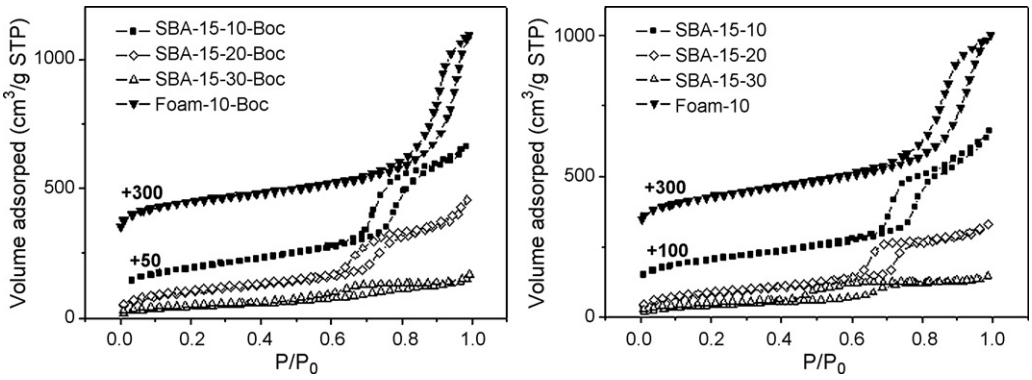

Fig. 3. Nitrogen sorption isotherms of L-prolinamide functionalized mesoporous silicas synthesized by co-condensation method before and after deprotection.

the mesopore [19]. Compared with SBA-n-Boc, no great change of *d* (1 0 0) spacings was observed for SAB-15-n (Table 1). The above results indicate that the mesostructural order of the materials does not deteriorate severely during the deprotection process.

In order to further confirm the structural order, the TEM technique was used for the characterization of SBA-15-n materials (Fig. 2). All SBA-15-n materials clearly showed parallel straight pores and hexagonally arrayed pores, which could be respectively ascribed to the (1 1 0) and (1 0 0) directions of p6 mm phase, suggesting that these materials had 2D hexagonal mesostructure in consistent with the XRD results. No XRD diffraction peaks were observed in the XRD pattern of Foam-10. The TEM images showed that this sample had disordered foam-like structure (Fig. S1).

The nitrogen sorption isotherms and pore size distribution curves of SBA-15-n-Boc and SBA-15-n are presented in Figs. 3 and S2, and the corresponding textural properties are summarized in Table 1. Before and after deprotection, all materials exhibited type IV isotherm patterns, suggesting the existence of mesoporosity. All SBA-15 type samples showed a sharp capillary condensation step with an H1 hysteresis loop at the relative pressure P/P_0 in the range of 0.4–0.83, suggesting that these materials had open cylindrical mesopore in line with the XRD results. With the concentration of PCA increasing, the capillary condensation step shifted to lower relative pressure, showing the decrease in the pore diameter (Table 1). It should be mentioned that the hysteresis loop at high relative pressure of P/P_0 above 0.9 may come from the interparticle void space. Foam-10 and Foam-10-Boc exhibited a type IV isotherm pattern with an H1 hysteresis loop at the relative pressure P/P_0 in the range of 0.8–1.0, suggesting that this material had a large pore size (Fig. 3). Foam-10 has bimodal pore structure with adsorption pore size of 28.3 and 13.8 nm (Fig. S3), a BET surface area of 464 m^2/g and a total pore volume of 1.09 cm^3/g, being very much alike the conventional MCF silicas synthesized from acidic TEOS mixtures in the presence of P123 with TMB as the oil phase [20]. The BET surface area, pore volume and pore diameter of the materials decreased sharply with the content of PCA in the initial mixture increasing for SBA-15-n-Boc and SBA-15-n. This is reasonable because of the geometrical constrictions to accommodate a large number of bulky organosilane PCA in the mesoporous walls [21]. Compared with SBA-15-n-Boc and Foam-10-Boc, the decrease in BET surface area and pore diameter was observed for SBA-15-n and Foam-10 after deprotection (Table 1).

The organosilane, PCA, was also grafted onto SBA-15 and MCM-41. The textural parameters are summarized in Table 1. XRD, N_2 sorption isotherms and pore size distribution of the materials before and after grafting could be found in Figs. S4–S6. The sharp decrease in the BET surface area and pore volume of the materials after grafting suggests the successful incorporation of PCA onto the support.

3.3. Composition characterization of L-prolinamide functionalized mesoporous materials

The FT-IR spectra of SBA-15-30-Boc and SBA-15-30 were recorded after evacuation at 150 °C for 2 h (Fig. 4). The C—H stretching vibrations of the aromatic ring appeared at 3073 and 3035 cm^{-1} [22]. The strong vibrational bands at 2935 and 2861 cm^{-1} in the FT-IR spectrum of SBA-15-30-Boc were assigned to the CH stretching of CH_2 of the L-prolinamide functional group. The C=O stretching vibration of the Boc group was observed at 1701 cm^{-1}. The peak at 1679 cm^{-1} was ascribed to the C=O stretching of amide. The N—H scissoring vibration at 1592 cm^{-1} was overlapped with the C=C stretching vibration of the aromatic ring at 1607 cm^{-1} [22]. The C=C deformation vibration of the aromatic ring was observed at 1530 cm^{-1}. The peak at 1453 cm^{-1} was the mixture of characteristic CH deformation vibration of diaminecyclohexene and L-prolinamide [23]. The CH deformation vibration of methyl in the Boc group appeared at 1365 and 1397 cm^{-1} [22]. After deprotection, a new peak at 1385 cm^{-1} corresponding to CH deformation vibration of α-carbon of amide was overlapped by the peak at 1397 cm^{-1} in SBA-15-30-Boc. The intensity of the C=O stretching band of the Boc group at 1701 and 1635 cm^{-1} together with the CH deformation vibration of methyl in the Boc group at 1397 and 1365 cm^{-1} decreased sharply after deprotection, which demonstrated that most of the Boc group could be removed from the material during the deprotection process [22].

The integrity of the organic group in SBA-15-30-Boc and SBA-15-30 was further characterized by solid-state ^{13}C CP-MAS NMR

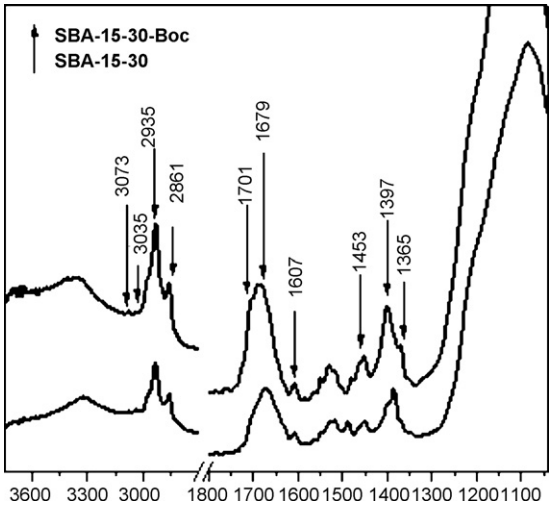

Fig. 4. FT-IR spectra of SBA-15-30 and SBA-15-30-Boc.

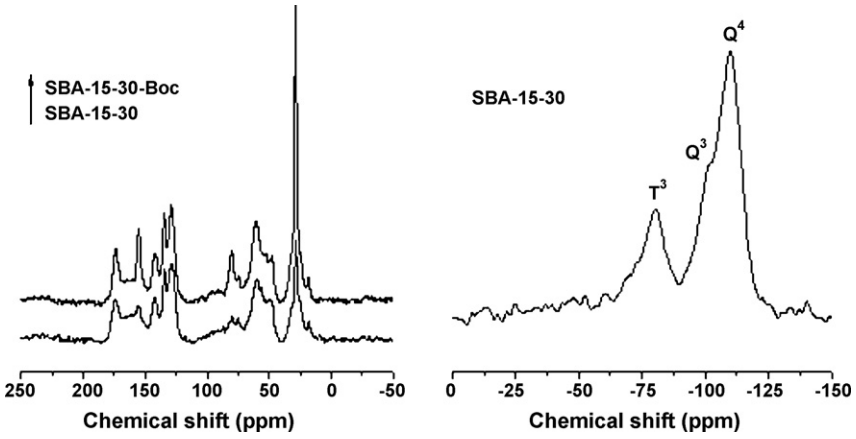

Fig. 5. Solid-state ^{13}C CP-MAS NMR (left) and ^{29}Si CP-MAS NMR (right) spectra of SBA-15-30-Boc and SBA-15-30.

(Fig. 5). The ^{13}C CP-MAS NMR spectra of SBA-15-30-Boc and SBA-15-30 displayed signals corresponding to cyclic CH_2 in the range of 20.0–30.0 ppm [23]. The signals at 48.3 and 60.4 ppm could be assigned to NCH and NCH_2, respectively. The existence of the phenyl group was confirmed by the signals at 129–155 ppm [23]. The signals at 174 ppm was ascribed to C=O of ester and amide. For SBA-15-30-Boc, the C—O signals of the Boc group appeared at 75–80 ppm and 20–30 ppm. The signals at 20–30 ppm were overlapped with the cyclic CH_2. Compared with SBA-15-30-Boc, SBA-15-30 showed a remarkably low intensity of signals assigned to Boc at 70–80 and 20–30 ppm decreased, suggesting that most of the Boc group was removed. The weak signals of Boc observed in the ^{13}C CP-MAS NMR spectrum of SBA-15-30 might be due to the group buried in the material walls, which could not be accessed by the deprotection agent. The NMR results, together with the FT-IR results, confirmed the incorporation of the L-prolinamide functional group in the mesoporous silicas and successful removal of most Boc groups during the deprotection process.

^{29}Si NMR spectrum of SBA-15-30 clearly showed both T and Q silicon sites (Fig. 5). The signals at −110.4 and −101.5 ppm arise from the Si species of Q^4 [$Si(OSi)_4$] and Q^3 [$Si(OH)(OSi)_3$], respectively. No signals of Q^2 and Q^1 were observed, suggesting the high condensation degree of the sample synthesized under the present synthetic conditions. The signal at −80.6 ppm can be assigned to T^3 [$SiC(OSi)_3$]. Integration results showed the ratio of $S_T/(S_T + S_Q) \approx 27\%$, suggesting that more than 90% organosilane in the initial mixture was incorporated into the network. The ^{29}Si NMR suggested that the present condition was an efficient method for the synthesis of hybrid mesoporous materials.

FT-IR results of SBA-15-*n* (*n* = 10, 20), Foam-10, G-SBA-15 and G-MCM-41 also confirmed the successful incorporation of the L-prolinamide functional group (Fig. S7).

3.4. Catalytic performance of L-prolinamide functionalized mesoporous materials

The design and synthesis of multifunctional chiral organocatalysts are of great academic interest because the catalytic activity and selectivity of a catalyst with two or more reactions promoting functionalities will be easily tuned by a simple modification of the structural motif of the catalyst. L-Proline and its derivatives, which are used as catalyst in asymmetric aldol reaction, Mannich reaction, Michael addition reaction and other reactions [1–3,24–28], is one of the most widely investigated organocatalyst. So we designed an organosilane precursor containing bifunctional groups based on L-proline. The catalytic performance of the materials was investigated in the direct asymmetric aldol reaction between 4-nitrobenzaldehyde and cyclohexanone.

Table 2 summarizes the content of L-prolinamide and the catalytic performance of the materials. It is interesting to mention that SBA-15-*n* samples synthesized by the co-condensation

Table 2
Direct asymmetric aldol reaction on L-prolinamide functionalized mesoporous materials[a].

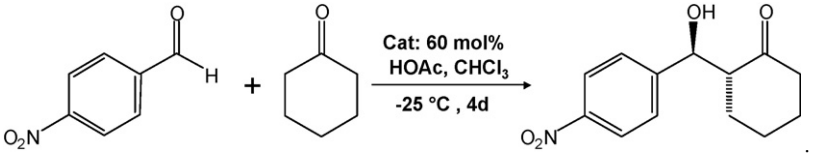

Sample	*N* (wt.%)	L-Prolinamide content[b] (mmol g^{-1})	Yield[c] (%)	Syn/anti[d]	ee (%)[d] anti/syn
SBA-15-10	2.68	0.64	87	11/89	90/12
SBA-15-20	4.22	1.00	86	30/70	91/42
SBA-15-30	5.35	1.27	89	30/70	87/42
Foam-10	2.04	0.33	85	13/87	75/24
G-SBA-15	1.39	0.33	83	21/79	88/59
G-MCM-41	1.69	0.40	85	20/80	88/16
SBA-15	–	–	N[e]	–	–
PCA	–	–	N[e]	–	–

[a] Reaction conditions: catalysts: 60 mol%, $CHCl_3$: 0.5 mL, cyclohexanone: 0.5 mL, HOAc: 4.3 μL, 4-nitrobenzaldehyde: 0.125 mmol, −25 °C, 4d.
[b] Based on elemental analysis.
[c] Isolated yield after separation by silica gel.
[d] Determined by HPLC.
[e] No reaction.

Table 3
The effect of amounts of acetic acid on direct asymmetric aldol reaction between cyclohexanone and 4-nitrobenzaldehyde on SBA-15-30[a].

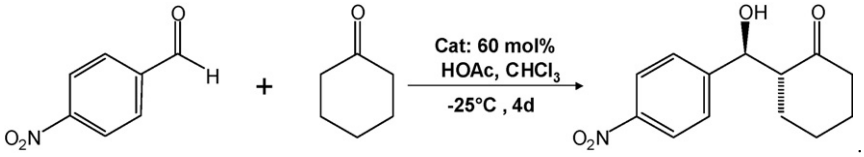

AcOH (μL)	Yield[b] (%)	Syn/anti[c]	ee[c] (%) anti/syn
0	35	36/64	40/19
2.2	67	25/75	86/33
4.3	87	30/70	87/42
8.6	75	18/82	93/46

[a] Reaction conditions: SBA-15-30: 60 mol%, $CHCl_3$: 0.5 mL, cyclohexanone: 0.5 mL, HOAc, 4-nitrobenzaldehyde: 0.125 mmol, −25 °C, 4d.
[b] Isolated yield after separation by silica gel.
[c] Determined by HPLC.

Table 4
The solvent effect on the direct asymmetric aldol reaction between cyclohexanone and 4-nitrobenzaldehyde on SBA-15-30[a].

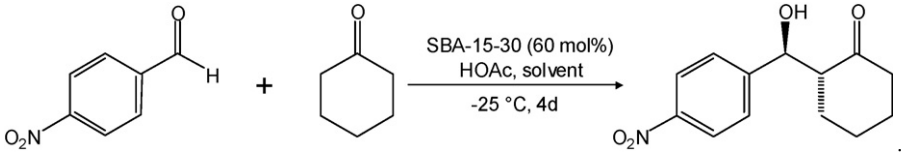

Solvents	Yield[b] (%)	Syn/anti[c]	ee[c] (%) anti/syn
$CHCl_3$	89	30/70	87/42
CH_2Cl_2	87	15/85	96/39
THF	87	24/76	87/39
Toluene	86	20/80	88/35
DMF	86	15/85	91/5

[a] Reaction conditions: SBA-15-30: 60 mol%, solvent: 0.5 mL, cyclohexanone: 0.5 mL, HOAc: 4.3 μL, 4-nitrobenzaldehyde: 0.125 mmol, −25 °C, 4d.
[b] Isolated yield after separation by silica gel.
[c] Determined by HPLC.

method had more amounts of L-prolinamide than G-SBA-15 and G-MCM-41 prepared by the grafting method, suggesting that the co-condensation was an effective method for the synthesis of hybrid materials. However, it was unexpected that Foam-10 had a much lower L-prolinamide content than SBA-15-10 while the initial content of PCA for the two samples was the same. This is probably because the hydrolysis and condensation rate of TEOS and PCA did not match in the absence of Na_2SiO_3.

Controlled experiment showed that the support, SBA-15, exhibited no catalytic activity for the aldol reaction. PCA also cannot catalyze the reaction due to the presence of Boc group (Table 2). All prolinamide containing samples showed catalytic activity and enantioselectivity in the direct aldol reaction of 4-nitrobenzaldehyde with cyclohexanone (Table 2). SBA-15-10 and SBA-15-20 gave similar ee values and activities. The highest ee value could reach as high as 91%, which was slightly higher than that obtained on G-SBA-15 and G-MCM-41 prepared by the grafting method, suggesting that the materials synthesized by the co-condensation method were efficient catalysts for aldol reaction and the chirality of L-prolinamide was not altered during the synthetic process. SBA-15-30 showed slightly lower ee value than SBA-15-10 or SBA-15-20, probably due to the low surface area and disordered mesostructure. G-SBA-15 and G-MCM-41 with different pore diameters had almost the same activity, ee value and syn/anti-ratio, indicating that the pore diameter had little influence on the catalytic performance of the catalyst under the present reaction conditions. Unexpectedly, the ee value of Foam-10 was the lowest among all materials investigated. This was probably due to the disordered mesostructure. The above results suggested that ordered pore structure endowed improved enantioselectivity.

To optimize the reaction conditions, the effect of the amounts of acetic acid was investigated by using SBA-15-30 as a representative catalyst (Table 3). Without the addition of HOAc, the yield, syn/anti-ratio and ee was very low. When 2.2 μL of HOAc was added to the reaction system, the yield increased from 35 to 67% accompanied by a sharp increase in ee (from 40 to 86%). Moreover, the syn/anti-ratio also increased to 25/75. The ee value increased with the amounts of HOAc and reached the highest of 93% as the amount of HOAc was increased to 8.6 μL. The product yield was first increased when the HOAc amounts was increased and reached the maximum at HOAc amounts of 4.3 μL. The catalytic results suggest that HOAc plays an important role in the reaction, as it may provide a proton to accelerate the formation of enamine. But the excessive HOAc may have a negative effect on the hydrogen bonding of diamide, which in turn depresses the catalytic efficacy [9].

Table 5
Direct asymmetric aldol reaction of aldehyde with cyclohexanone on SBA-15-30[a].

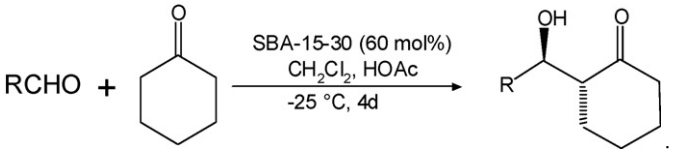

R	Yield[b] (%)	Syn/anti[c]	ee[c] (%) anti/syn
4-NO_2Ph	87	15/85	96/39
2-NO_2Ph	70	22/78	81/50
3-NO_2Ph	81	21/79	82/35
4-CNPh	78	27/73	76/44
4-CF_3Ph	<10	n.d.	

[a] Reaction conditions: SBA-15-30: 60 mol%, CH_2Cl_2: 0.5 mL, cyclohexanone: 0.5 mL, HOAc: 4.3 μL, aldehyde: 0.125 mmol, −25 °C, 4d.
[b] Isolated yield after separation by silica gel.
[c] Determined by HPLC.

Table 6
The recycle results of SBA-15-30 in the direct asymmetric aldol reaction between cyclohexanone and 4-nitrobenzaldehyde[a].

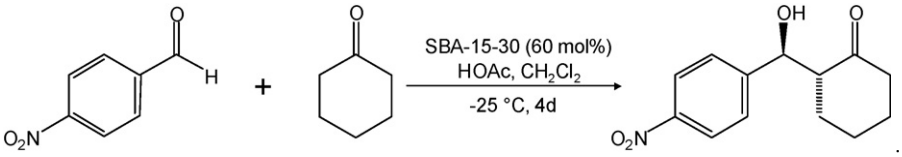

Entry	Yield[b] (%)	Syn/anti[c]	ee[c] (%)
1	87	15/85	96/39
2	88	20/80	94/64
3	87	26/74	95/34
4	87	53/47	87/69

[a] Reaction conditions: SBA-15-30: 60 mol%, CH_2Cl_2: 1.0 mL, cyclohexanone: 1.0 mL, HOAc: 8.6 μL, aldehyde: 0.25 mmol, −25 °C, 4d.
[b] Isolated yield after separation by silica gel.
[c] Determined by HPLC.

The solvent also played important role in the catalytic performance of the materials (Table 4). The product yield remained almost the same in organic solvents examined, but the solvent effect on the stereoselectivity was observed. The highest enantioselectivity (96% ee for the major anti-isomer) was achieved in CH_2Cl_2. Under optimized conditions, the catalytic performance of SBA-15-30 was also tested in aldol reactions using different kinds of substrate (Table 5, all the aldol products in Table 5 are known products [3]). Compared with 4-nitrobenzaldehyde, the yield, syn/anti-ratio and ee were lower when 2-nitrobenzaldehyde and 3-nitrobenzaldehyde were used. The ee was only 76% when 4-cyanobenzaldehyde was used. For 4-(trifluromethyl)benzaldehyde, the catalyst exhibited very low catalytic activity. The above results showed that the best substrate for SBA-15-30 was 4-nitrobenzaldehyde.

To prove the heterogeneous nature of the supported catalysts, two parallel reactions of cyclohexhanone with 4-nitrobenzaldehyde were allowed to carry on for 2 days. One reaction was stopped, and the isolated yield of the product was 54%. In the other reaction, the catalyst, SBA-15-30, was filtered off. The reaction in homogeneous was allowed to continue. After another 2 days, the isolated yield of the product was 57%. The result indicated that the reaction proceeded very slowly without the heterogeneous catalyst.

In the direct aldol reaction of 4-nitrobenzaldehyde with cyclohexanone, the catalyst could be used three times without obvious loss of reaction yield and ee value (Table 6). For the fourth cycle, a slight decrease in ee was observed, which may be due to the deactivation of L-prolinamide during the catalytic process. However, we cannot explain the decrease in the syn/anti-ratio when the catalyst was reused.

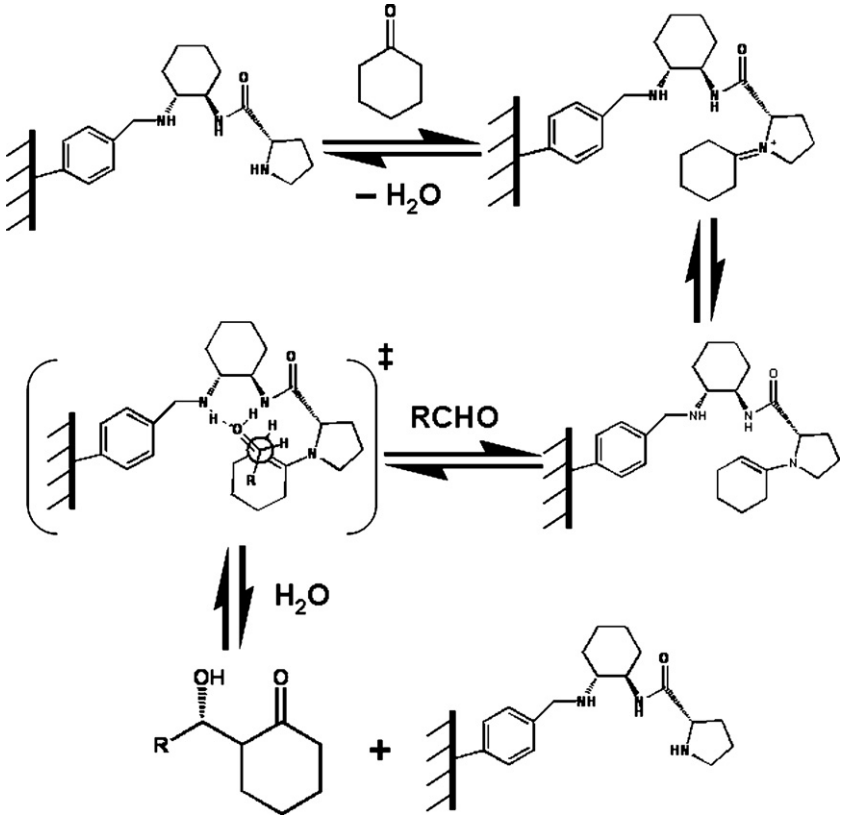

Scheme 2. Proposed mechanism of the direct asymmetric aldol reaction catalyzed by SBA-15-n.

3.5. Proposed mechanism of the reaction

The mechanism of aldol reaction is the subject of an extensive investigation. Here we assume that the PCA-functionalized mesoprous materials-catalyzed aldol reactions conform to the generally accepted syn-enamine mechanism based on previous reports (Scheme 2) [29–32]. In the transition state, the aldehyde is activated by hydrogen bonding with the NH of the catalyst in a manner such that C—C bond formation takes place from its *re* face, and then the product can be obtained after hydrolysis [32,33].

4. Conclusions

In summary, we have successfully synthesized L-prolinamide functionalized mesoporous silicas with ordered hexagonal and disordered foam-like structure in weak acid HOAc–NaOAc buffer solution. Higher amounts of organic groups could be incorporated in the material by the co-condensation method than by the grafting method. The results of FT-IR and NMR characterizations show that the organofunctional group remains intact during the synthetic process. The materials show catalytic activity and enantioselectivity in the direct asymmetric aldol reaction between 4-nitrobenzaldehyde and cyclohexanone. The highest ee value could reach as high as 96%. The materials prepared by the co-condensation method exhibit similar activity and enantioselectivity to that by the grafting method. As chiral amine has been widely investigated in various organocatalysis fields, our catalyst may also be efficient for other enamine catalysis reaction.

Acknowledgements

Financial support of this work was provided by the National Natural Science Foundation of China (20621063, 20673113), 973 Project (2009CB623503) and Programme Strategic Scientific Alliances between China and the Netherlands (2008DFB50130).

Appendix A. Supplementary data

Supplementary data associated with this article can be found, in the online version, at doi:10.1016/j.molcata.2009.08.005.

References

[1] B. List, R.A. Lerner, C.F. Barbas III, J. Am. Chem. Soc. 122 (2000) 2395.
[2] S. Mukherjee, J.W. Yang, S. Hoffmann, B. List, Chem. Rev. 107 (2007) 5479.
[3] S.Z. Luo, J.Y. Li, L. Zhang, H. Xu, J.P. Cheng, Chem. Eur. J. 14 (2008) 1273.
[4] L. Zhong, J.L. Xiao, C. Li, J. Catal. 243 (2006) 442.
[5] K. Yamaguchi, T. Imago, Y. Ogasawara, J. Kasai, M. Kotani, N. Mizuno, Adv. Synth. Catal. 348 (2006) 1516.
[6] P. Yu, J. He, C.X. Guo, Chem. Commun. (2008) 2355.
[7] F. Calderón, R. Fernández, F. Sánchez, A. Fernández-Mayoralas, Adv. Synth. Catal. 347 (2005) 1395.
[8] E.A. Prasetyanto, S.-C. Lee, S.-M. Jeong, S.-E. Park, Chem. Commun. (2008) 1995.
[9] J.-R. Chen, H.-H. Lu, X.-Y. Li, L. Cheng, J. Wan, W.-J. Xiao, Org. Lett. 7 (2005) 4545.
[10] D. Jiang, Q.H. Yang, H. Wang, G. Zhu, J. Yang, C. Li, J. Catal. 239 (2006) 65.
[11] D. Zhao, Q. Huo, J. Feng, B.F. Chmelka, G.D. Stucky, J. Am. Chem. Soc. 120 (1998) 6024.
[12] J. Liu, J. Yang, Q.H. Yang, G. Wang, Y. Li, Adv. Funct. Mater. 15 (2005) 1297.
[13] J. Liu, Q.H. Yang, X.S. Zhao, L. Zhang, Micropor. Mesopor. Mater. 106 (2007) 62.
[14] Y. Wan, D.Y. Zhao, Chem. Rev. 107 (2007) 2821.
[15] T. Asefa, M. Kruk, M.J. Maclachlan, N. Coombs, H. Grondey, M. Jaroniec, G.A. Ozin, J. Am. Chem. Soc. 123 (2001) 8520.
[16] Q. Yang, M.P. Kapoor, S. Inagaki, J. Am. Chem. Soc. 124 (2002) 9694.
[17] M.C. Burleigh, M.A. Markowitz, M.S. Spector, B.P. Gaber, J. Phys. Chem. B 105 (2001) 9935.
[18] M.C. Burleigh, S. Dai, E.W. Hagaman, J.S. Lin, Chem. Mater. 13 (2001) 2537.
[19] F. Martínez, G. Morales, A. Martín, R. van Gridken, Appl. Catal. A 347 (2008) 169.
[20] P. Schmidt-Winkel, W.W. Lukens, D. Zhao, P. Yang, B.F. Chmelka, G.D. Stucky, J. Am. Chem. Soc. 121 (1999) 254.
[21] L. Zhang, J. Liu, J. Yang, Q.H. Yang, C. Li, Micropor. Mesopor. Mater. 109 (2008) 172.
[22] G. Socrates, Infrared Characteristic Group Frequencies. Tables and Charts, 2nd ed., Wiley, Chichester, 1994, p. 62. 237.
[23] D.M. Jiang, J.S. Gao, Q.H. Yang, J. Yang, C. Li, Chem. Mater. 18 (2006) 6012.
[24] A. Dondoni, A. Massi, Angew. Chem. Int. Ed. 47 (2008) 2.
[25] B.M. Trost, L.R. Terrell, J. Am. Chem. Soc. 125 (2003) 338.
[26] L. He, Z. Tang, L.F. Cun, A.Q. Mi, Y.Z. Jiang, L.Z. Gong, Tetrahedron 62 (2006) 346.
[27] H. Huang, E.N. Jacobsen, J. Am. Chem. Soc. 128 (2006) 7170.
[28] J.W. Yang, C. Chanlder, M. Stadler, D. Kampen, B. List, Nature 452 (2008) 453.
[29] K. Sakthivel, W. Notz, T. Bui, C.F. Barbas III, J. Am. Chem. Soc. 123 (2001) 5260.
[30] M. Nakadai, S. Saito, H. Yamamoto, Tetrahedron 58 (2002) 8167.
[31] S.Z. Luo, X.L. Mi, L. Zhang, S. Liu, H. Xu, J.P. Cheng, Tetrahedron 63 (2007) 1923.
[32] Z. Tang, Z.H. Yang, X.H. Chen, L.F. Cun, A.Q. Mi, Y.Z. Jiang, L.Z. Gong, J. Am. Chem. Soc. 127 (2005) 9285.
[33] V. Maya, M. Raj, V.K. Singh, Org. Lett. 9 (2007) 2593.